

Published in final edited form as:

Proc Combust Inst. 2013 January ; 34(1): 297–305. doi:10.1016/j.proci.2012.06.005.

Low temperature oxidation of benzene and toluene in mixture with *n*-decane

Olivier Herbinet, Benoit Husson, Maude Ferrari, Pierre-Alexandre Glaude, and Frédérique Battin-Leclerc*

Laboratoire Réactions et Génie des Procédés, CNRS, Université de Lorraine, 1 rue Grandville, 54000 Nancy, France

Abstract

The oxidation of two blends, benzene/*n*-decane and toluene/*n*-decane, was studied in a jet-stirred reactor with gas chromatography analysis (temperatures from 500 to 1100 K, atmospheric pressure, stoichiometric mixtures). The studied hydrocarbon mixtures contained 75% of aromatics in order to highlight the chemistry of the low-temperature oxidation of these two aromatic compounds which have a very low reactivity compared to large alkanes. The difference of behavior between the two aromatic reactants is highly pronounced concerning the formation of derived aromatic products below 800 K. In the case of benzene, only phenol could be quantified. In the case of toluene, significant amounts of benzaldehyde, benzene, and cresols were also formed, as well as several heavy aromatic products such as bibenzyl, phenylbenzylether, methylphenylbenzylether, and ethylphenylphenol. A comparison with results obtained with neat *n*-decane showed that the reactivity of the alkane is inhibited by the presence of benzene and, to a larger extent, toluene. An improved model for the oxidation of toluene was developed based on recent theoretical studies of the elementary steps involved in the low-temperature chemistry of this molecule. Simulations using this model were successfully compared with the obtained experimental results.

Keywords

Benzene; Toluene; Decane; Low-temperature oxidation; Jet-stirred reactor

1. Introduction

Despite the abundance of experimental studies and models concerning the oxidation of neat benzene and toluene [1], their reactivity below 900 K is still poorly known since these compounds are unreactive below 900 K. The low-temperature oxidation of aromatics might however be initiated by the reaction of a species with a higher reactivity, such as *n*-alkane. This is what actually happens during the oxidation of alkane/aromatic mixtures which are often proposed as gasoline surrogates [1].

Studies on the low-temperature oxidation of mixtures of light aromatics with more reactive fuel components have mainly concerned global reactivity at high temperature, such as ignition delay times in shock tubes [2], [3], [4] and [5], in a rapid compression machine [6] and in a HCCI engine [7]. The fuel consumption and the formation of some main combustion products have also been investigated in jet-stirred [5] and [8] and flow [9]

*Corresponding author: Frédérique BATTIN-LECLERC, Laboratoire Réactions et Génie des Procédés, Ecole Nationale Supérieure des Industries Chimiques, BP 20451, 1 rue Grandville, 54000 Nancy, France, Tel: +33 (0)3 83 17 51 25, Fax: +33 (0)3 83 17 81 20, frederique.battin-leclerc@univ-lorraine.fr.

reactors. Very little attention has been given to mixtures including benzene [6], or to the formation of products obtained via the consumption of the aromatic reactants. Yahyaoui et al. [5] have given a detailed speciation of the products obtained from the oxidation in a jet-stirred reactor at 10 atm of an iso-octane/toluene/1-hexene/ethyltert-butylether blend, but only at temperatures above 800 K, i.e. beyond the negative temperature coefficient (NTC) region. Lenhert et al. [9] have identified benzaldehyde, benzene and phenol as the aromatic products obtained from the oxidation in a flow reactor of a *n*-heptane/*iso*-octane/1-pentene/toluene blend between 600 and 800 K at 8 atm.

The purpose of this paper is to investigate experimentally the low-temperature oxidation of benzene and toluene below and in the NTC region (500–1100 K) using a jet-stirred reactor with identification and quantification of the reaction products. Experiments have been performed in the presence of *n*-decane, an alkane with a high reactivity at low temperature. *n*-Decane was used rather than smaller *n*-heptane to avoid problem of peak separations in chromatographic analyses due to the use of two C₇ reactants. The second purpose of this paper is to model the low temperature oxidation chemistry of benzene and toluene by taking into account recent theoretical studies of the elementary steps involved in the low-temperature chemistry of aromatic compounds.

2. Experiments

The reactor used in this study was a fused silica spherical jet-stirred reactor operated at constant temperature and pressure, which has often been used for gas phase kinetic studies [10] and [11]. It is composed of a sphere with an injection cross located at its center. The mixing of the gas-phase inside the reactor is achieved through turbulent jets issued from the four nozzles of the cross. In order to avoid the formation of temperature gradients (never more than 5 K) in the gas phase, the reactor is preceded by an annular preheater in which the temperature of the gas mixture is increased progressively to the reaction temperature.

The fuel flow rate was controlled by a liquid mass flow controller, mixed to the carrier gas and then evaporated by passing through a single pass heat exchanger, the temperature of which was set above the boiling point of the mixture. Carrier gas and oxygen flow rates were controlled by gas mass flow controllers with an accuracy on liquid and gas mass flow rates of around 0.5%.

Reaction products were analyzed on-line using four gas chromatographs. A first chromatograph (Carbosphere packed column, thermal conductivity detection (TCD) and flame ionization detection (FID)), was used for the quantification of O₂, CO, CO₂ and methane. A second gas chromatograph (Plot Q capillary column and FID) was used for the quantification of C₁–C₄ hydrocarbons and light oxygenated compounds. Hydrogen, water and formaldehyde were not quantified. A third chromatograph (HP-1 capillary column and FID) was used to analyze hydrocarbons and oxygenated species with more than five heavy atoms. As it was not in the scope of this paper, large compounds deriving from *n*-decane have not been quantified. A fourth gas chromatograph (HP-1 or Plot Q capillary column, mass spectrometry detection) was used for identification. The calibration was performed by injecting known amounts of the pure substances when available, otherwise the method of the effective carbon number was used (species having the same number of carbon atoms and the same functional groups were assumed to have the same response in the FID). The detection threshold was about 100 ppb for the heaviest species (FID) and about 100 ppm for carbon oxides and oxygen (TCD). Uncertainty estimates on obtained mole fractions were about ± 5%.

The oxidation of stoichiometric *n*-decane/benzene and *n*-decane/toluene blends was studied in the above described reactor over the temperature range 550–1100 K, at a pressure of 106

kPa (800 Torr), at a residence time of 2 s. The mixtures were diluted in helium (fuel mole fraction of 0.01 with 75% of aromatics). Benzene, toluene and *n*-decane were provided by Sigma-Aldrich (purity ~ 99.9%), VWR (purity ~ 99.99%), and Fluka (purity ~ 98%), respectively. Helium and oxygen were purchased from Messer (purity of 99.999% for He and of 99.995 for O₂), respectively. In both sets of experiments, the initial mole fractions of *n*-decane and aromatic compounds were taken equal to 0.0025 and 0.0075, respectively. In order to compare the impact of benzene and toluene on the reactivity, the oxidation of neat *n*-decane was also performed under the same conditions with benzene and toluene replaced by helium (equivalence ratio of 0.41). Tables presenting the obtained experimental data are available as Supplementary Data.

Figure 1 presents the evolution with temperature of the mole fractions of the two aromatic reactants (Fig. 1a) and of the major obtained aromatic products. The names and the structures of all the aromatic products detected in this study are given in Table 1. A negligible conversion of benzene is observed below 880 K, and the only quantified aromatic compound obtained from benzene at low temperature is phenol (Fig. 1a). Due to the reactivity of *n*-decane, the formation of phenol displays an NTC behavior between 700 and 800 K, traces of bibenzyl and toluene were also detected. At higher temperatures, ortho- and para-cresols were also quantified (maximum mole fraction of 70 ppm at 950 K for each isomer).

Figure 1 shows a significant conversion of toluene between 550 and 800 K (maximum of 23% at 650 K), with a marked NTC behavior between 700 and 800 K. The main aromatic compound formed at low temperature from toluene is benzaldehyde (Fig. 1b, 400 ppm at 650 K), with smaller amounts of benzene (Fig. 1b, 100 ppm), phenol (Fig. 1b, 150 ppm) and cresols (Fig. 1b, 60 ppm). The three major aromatic species observed above 800 K are benzaldehyde, phenol and cresols (Fig. 1b, 550, 1600 and 200 ppm, respectively, at 900 K). Above 800 K, the formation of small amounts (below 100 ppm at 900 K) of ethylbenzene (Fig. 1c), styrene (Fig. 1c), 1-butenylbenzene (Fig. 1c), and benzofuran is also observed. Note that benzaldehyde, benzene and phenol were also the main aromatic products observed by Lenhert et al. [9] during the low-temperature oxidation of a blend including alkanes and toluene.

Figure 2 presents the evolution with temperature of the *n*-decane mole fraction in the three cases studied. In all the figures showing experiments and simulations, points represent experiments and lines model predictions. Below 800 K, the addition of benzene has a very slight inhibiting effect on *n*-decane oxidation, while that of toluene has a more marked impact. Above 800 K, the presence of each aromatic compound has a similar inhibiting influence.

The same non-aromatic products have been observed in our previous studies of the oxidation on *n*-decane in the same reactor [10] and [11] (see complete experimental data in Supplementary Data). Since the formation of these products is mostly influenced by the oxidation of *n*-decane, Fig. 3 presents the mole fractions of oxygen and only the main of these products. In order to see the low-temperature behavior more precisely, these figures are plotted from 500 to 900 K. Compared to neat *n*-decane, almost no effect of the addition of benzene is observed on the formation of C₀-C₅ products below 800 K. In presence of toluene with the same initial *n*-decane mole fraction, the formation of carbon monoxide at 650 K is reduced by 50%, that of acetaldehyde by 12%, that of 1-butene by a factor 1.5 and those of ethylene and propene by a factor of 2. These changes are due both to the inhibiting influence of toluene on the conversion of *n*-decane and to the degradation of toluene. Above 800 K, the maxima of the mole fractions of products, such as acetaldehyde, ethylene and propene, occur at higher temperature in the blends than in pure *n*-decane.

In order to analyze heavy compounds formed during the low-temperature oxidation of the *n*-decane/toluene blend, the gas leaving the reactor was condensed in a trap maintained at liquid nitrogen temperature. After a given period of time, the trap was disconnected and acetone (solvent) and a known amount of *n*-octane acting as internal standard were added. When the temperature of the trap was close to room temperature, the liquid mixture in the trap was poured into a sampling bottle and then injected in the chromatographs fitted with a HP1 column.

Figure 4 presents the evolution with temperature of the mole fractions of the major low-temperature products quantified by this method: bibenzyl, phenylbenzylether, methylphenylbenzylether, and ethylphenylphenol. Here also, due to the reactivity of *n*-decane, the evolutions of all these compounds display a marked NTC behavior. Compounds formed only above 800 K include stilbene, naphthalene, methoxybenzene, and phenanthrene. Other compounds were detected but not quantified, these include: benzylalcohol, hydroxybenzadehyde, and hydroxyphenol.

3. Modeling

An improved mechanism for the oxidation of toluene has been added to the model proposed by Biet et al. [10] for the low-temperature oxidation of *n*-decane. The global mechanism for the mixture involves 4201 reactions and includes 663 species and is available as Supplementary Data on the website of this journal in CHEMKIN format [12].

3.1. General description of the model

Thermochemical data were mainly estimated by the software THERGAS [13], which is based on the group additivity methods proposed by Benson [14], apart from the heat of formation of some species (see comments in the provided mechanism), which were taken from Goos et al. [15] (that is the case of biaromatic species) or re-evaluated using quantum calculations performed by Gaussian03 [16] at the CBS-QB3 level of theory [17].

The model of toluene is an up-date of that of Gueniche et al. [18] which includes:

- A primary and a secondary mechanism of the oxidation of toluene [19]. This toluene mechanism [19] has also been used as a basis for an up-dated version by Metcalfe et al. [20], but with validations only above 900 K.
- A primary and a secondary mechanism of the oxidation of benzene [21]. The primary mechanism for toluene includes reactions of toluene and of benzyl, tolyl (methylphenyl), peroxybenzyl, benzoxyl and cresoxy free radicals, and that for benzene contains the reactions of benzene and of cyclohexadienyl, phenyl, phenylperoxy, phenoxy, hydroxyphenoxy, cyclopentadienyl, cyclopentadienoxy and hydroxycyclopentadienyl free radicals.
- A mechanism for the oxidation of unsaturated C₃–C₄ species (the C₀–C₂ reaction base is common to the mechanisms of toluene and of *n*-decane). In these reaction bases, pressure-dependent rate constants follow Troe's formalism and efficiency coefficients have been included.

When coupling both mechanisms, H-abstraction reactions from toluene by decylperoxy radicals, as well as those from *n*-decane by benzyl and methylphenyl radicals, have been considered.

3.2. Changes made in the mechanisms of benzene and toluene

Compared to the mechanism of Gueniche et al. [18], the rate constants proposed by Tian et al. [22] to model toluene flames have been used. The changes made in the low-temperature

oxidation mechanism of aromatic compounds are detailed hereafter. The changes made in both primary mechanisms are given in Table 2. It has been verified that these changes do not alter simulations for neat benzene [20] and toluene [19] (see Supplementary Data).

As far as the primary mechanism of benzene is concerned, Da Silva and Bozzelli [23] investigated the reaction pathways of phenyl radicals with O₂ molecules going via the formation of phenylperoxy radicals. We have considered these reactions (reactions (1)–(3) in Table 2), as well as the disproportionation of phenylperoxy radicals with HO₂ radicals and the subsequent decomposition of the obtained hydroperoxide to give phenoxy and OH radicals (reactions (4) and (5)).

In the case of the primary mechanism of toluene, we have used the rate constant of Baulch et al. [24] instead of that considered by Tian et al. [22] (i.e. the recent value of Oehlschlaeger et al. [31] which is in good agreement with the most recent recommendation of Baulch et al. [32]) for the bimolecular initiation between toluene and oxygen molecules (reaction (6)). The more recent values [31,32] were based on measurements performed above 1000 K and led to an underestimation of the reactivity in the case of the oxidation of neat toluene in a jet-stirred reactor (around 900 K, atmospheric pressure, $\Phi = 0.9$) [19]. Additional H-atom abstractions from toluene and combinations involving benzyl radicals have been included (reactions (7)–(11)). Da Silva and Bozzelli [26] investigated the kinetics of the reactions of benzylhydroperoxide via combination of benzyl and HO₂ radicals using quantum calculations. They showed that benzylhydroperoxide decomposes almost exclusively to yield benzoyl and OH radicals over a wide range of temperatures. Da Silva and Bozzelli [27] also studied the reaction pathways of the benzoyl radical. Low-energy pathways leading to benzaldehyde + H, to phenyl radical + formaldehyde and to benzene + formyl radical were highlighted. These reactions were added (reactions (12)–(17)), as well as reactions of methylphenyl radicals with O₂ molecules [23] (reactions (18)–(20)) and of benzylperoxy radicals with H-atoms [28] (reactions (21)–(23)). Note that reactions (15) and (17) were already considered in the mechanism of Gueniche et al. [18], but with fitted rate constants.

Amongst the heavy aromatic products experimentally detected in this study, only bibenzyl and stilbene molecules were considered by Bounaceur et al. [19]. Note that in the present study many of these products contain oxygen and are specific to low-temperature chemistry.

Bibenzyl are formed by combination of benzyl radicals and consumed by H-abstraction to give the resonantly stabilized C₁₄H₁₃ radical which can decompose into hydrogen atoms and stilbene. These reactions have been kept here, but the ipso-additions of H-atoms and OH radicals to bibenzyl, the reactions of C₁₄H₁₃ radicals with oxygen molecule yielding stilbene, the combination of C₁₄H₁₃ radicals with HO₂ radicals to give a hydroperoxide which decomposes to benzaldehyde, OH and benzyl radicals, as well as the consumption pathways of stilbene by additions of H-atoms and OH radicals, have been added. The formation of phenylbenzylether has been considered by ipso-addition of benzoyl radicals to toluene and by combination of phenoxy and benzyl radicals, that of methylphenylbenzylether by combination of cresoxy and benzyl radicals and of benzoyl and methylphenyl radicals, as well as that of 1-butenylbenzene by combination of allyl and benzyl radicals. Ethylphenylphenol is produced by combination of hydroxybenzyl and benzyl radicals and of hydroxyphenyl and phenylethyl radicals, but also by ipso-addition of OH radicals to bibenzyl. Consumption pathways of all these molecules through ipso-additions of H-atoms and H-abstractions followed by decompositions have been written. All these reactions with the associated kinetic data are documented in Supplementary Data. Note that all the kinetic data related to this last paragraph are based on estimation and are of considerable uncertainty.

4. Discussion

Simulations were performed with the PSR software of CHEMKIN [12]. In the case of neat *n*-decane, Fig. 2 and Fig. 3 show that this model reproduces well the consumption of fuel and oxygen, as well as the formation of the major light products (more simulations are shown as Supplementary Data). Figure 2 also shows that the model gives acceptable agreement of the influence of the addition of aromatic compounds on the reactivity of *n*-decane, even if the inhibiting effect of toluene is underestimated between 600 and 750 K. Figure 3 shows that the model simulates well the observed decrease in the formation of light products, apart from CO, in presence of aromatic compounds below 800 K. At higher temperatures, the shift in temperature in the maximum mole fractions in presence of aromatic compounds is also reproduced well.

Figure 1a shows that the consumption of benzene and toluene is well predicted by the model, as well as the formation of phenol in the case of the benzene blend. In the case of the toluene blend, the formation of benzene, benzaldehyde, ethylbenzene and styrene, is well predicted, while that of phenol and cresols is significantly overestimated below 800 K and that of 1-butenylbenzene is underestimated above 800 K. As shown in Fig. 4, the model leads to a good qualitative prediction of the heavy products deriving from toluene which are formed at low temperature. None can expect more than a qualitative agreement for such products due to uncertainties in both experimental measurements (condensation) and in the model given that reactions and the corresponding rate constants are mostly unknown.

A flow rate analysis has been performed for the two blends at 650 K under the conditions of Fig. 1. In the case of benzene, this analysis shows that phenol is formed from the reaction between HO₂ and phenoxy radicals; these last radicals deriving from phenylperoxy radicals via reaction (3). Phenylperoxy radical are obtained by addition to oxygen of phenyl radicals obtained directly from benzene by H-abstractions. In the toluene blend, the main reactions consuming the aromatic reactant are displayed in Fig. 5. Under these conditions, 78% of toluene is consumed by H-atom abstractions to form the resonantly stabilized benzyl radicals, and 14% to give methylphenyl radicals. Benzyl radicals react mainly by combination with HO₂ radicals to give benzyl hydroperoxide which decompose to benzoyl radicals which mostly decompose to benzaldehyde and H-atoms, and, for a very small fraction, benzene and CHO radicals. Benzaldehyde reacts mainly by H-atom abstractions yielding benzoyl radicals which readily decompose to give carbon monoxide and phenyl radicals, which are the source of phenol through the same pathway as when benzene is used as a reactant. Reacting as phenyl radicals, methylphenyl radicals are the source of cresols. The large existing uncertainties on the reactions pathways and the rate constants of benzoyl, phenoxy, methylphenyl and cresoxy radicals certainly explain the deviations observed between experiments and modeling for phenol and cresols.

Ethylbenzene, the source of styrene, and 1-butenylbenzene derive from combinations of benzyl radicals with methyl and allyl radicals, respectively. Phenylbenzylether is obtained by combination of phenoxy and benzyl radicals. The large overprediction of this species derives certainly from the same problem as the large overprediction of phenol. Methylphenylbenzylether derives from the combination of cresoxy and benzyl radicals. Ethylphenylphenol is obtained mainly by combination of hydroxybenzyl and benzyl radicals, and to a lesser extent by ipso-addition of OH radicals to bibenzyl, this molecule being mostly consumed by H-atom abstractions.

The formation of benzyl radicals by H-atom abstractions, which react mainly by combination reactions, especially to give bibenzyl, explains the inhibiting effect of toluene on the *n*-decane oxidation predicted below 600 K. In this temperature range, the additions of

decyl and hydroperoxydecyl radicals to oxygen are favored and promote the formation of ketohydroperoxides and the derived branching steps. On the other hand, the addition of benzyl radicals to oxygen is of very minor importance and does not lead to hydroperoxides. At higher temperatures, the additions to oxygen become reversible and the formation of unreactive HO₂ radicals is then favored instead of that of branching agents. In this temperature zone, the combination of benzyl and HO₂ radicals yielding benzylhydroperoxide, a branching agent, has then a promoting effect explaining the small predicted inhibiting effect of toluene.

5. Conclusion

This paper presents the first experimental study of the oxidation of benzene and toluene at low-temperature, i.e. between 550 and 800 K, with the aromatic compound as the major reactant and a detailed product analysis. These results have been obtained by using *n*-decane, a compound with a high reactivity at low-temperature, in order to trigger the reactions of the aromatic compounds. These results have allowed the validation of a new model which contains most of the recent reactions pathways for aromatic oxygenated radicals calculated using quantum mechanics method [23], [26], [27] and [28]. This model predicts the mole fractions of aromatic reactants and of main products well, but improvements are still needed in order to better reproduce the inhibiting effect of toluene in the NTC zone.

Supplementary Material

Refer to Web version on PubMed Central for supplementary material.

Acknowledgments

This study was supported by the European Commission through the “Clean ICE” Advanced Research Grant of the European Research Council. The authors thank S. Bax and O. Frottier for their help in performing toluene experiments.

References

- [1]. Battin-Leclerc F. *Prog. Energy Combust. Sci.* 2008; 34:440–498.
- [2]. Gauthier BM, Davidson DF, Hanson RK. *Combust. Flame.* 2004; 139:300–311.
- [3]. Herzler J, Fikri M, Hitzbleck K, et al. *Combust. Flame.* 2007; 149:25–31.
- [4]. Fikri M, Herzler J, Starke R, Schulz C, Roth P, Kalghatgi GT. *Combust. Flame.* 2008; 152:276–281.
- [5]. Yahyaoui M, Djebaili-Chaumeix N, Dagaut P, Paillard CE, Gail S. *Proc. Combust. Inst.* 2007; 31:385–391.
- [6]. Vanhove G, Petit G, Minetti R. *Combust. Flame.* 2006; 145:521–532.
- [7]. Andrae JCG, Björnbohm P, Cracknell RF, Kalghatgi GT. *Combust. Flame.* 2007; 149:2–24.
- [8]. Dubreuil A, Foucher F, Mounaïm-Rousselle C, Dayma G, Dagaut P. *Proc. Combust. Inst.* 2007; 31:2879–2889.
- [9]. Lenhert DB, Miller DL, Cernansky NP, Owens KG. *Combust. Flame.* 2009; 156:549–564.
- [10]. Biet J, Hakka MH, Warth V, Glaude P, Battin-Leclerc F. *Energy Fuels.* 2008; 22:2258–2269.
- [11]. Hakka MH, Glaude PA, Herbinet O, Battin-Leclerc F. *Combust. Flame.* 2009; 156:2129–2144.
- [12]. Kee, RJ.; Rupley, FM.; Miller, JA. Report S 89-8009B. Sandia Laboratories; 1993.
- [13]. Muller C, Michel V, Scacchi G, Côme GM. *J. Chem. Phys.* 1995; 92:1154.
- [14]. Benson, SW. *Thermochemical Kinetics.* second ed.. Wiley; New York: 1976.

- [15]. Goos, E.; Burcat, A.; Ruscic, B. Br. Ideal Gas Thermochemical Database with updates from Active Thermochemical Tables. Sep 12. 2011 available at <ftp://ftp.technion.ac.il/pub/supported/aetdd/thermodynamics>
- [16]. Frisch, MJ.; Trucks, GW.; Schlegel, HB., et al. Gaussian03, Revision D02. Gaussian, Inc.; Wallingford, CT: 2004.
- [17]. Montgomery JA, Frisch MJ, Ochterski JW, Petersson GA. J. Chem. Phys. 1999; 110:2822–2827.
- [18]. Gueniche HA, Biet J, Glaude PA, Fournet R, Battin-Leclerc F. Fuel. 2009; 88:1388–1393.
- [19]. Bounaceur R, Da Costa I, Fournet R, Billaud F, Battin-Leclerc F. Int. J. Chem. Kinet. 2005; 37:25–49.
- [20]. Metcalfe WK, Dooley S, Dryer FL. Energy Fuels. 2011; 25:4915–4936.
- [21]. Da Costa I, Fournet R, Billaud F, Battin-Leclerc F. Int. J. Chem. Kinet. 2003; 35:503–524.
- [22]. Tian ZY, Pitz WJ, Fournet R, Glaude PA, Battin-Leclerc F. Proc. Combust. Inst. 2011; 33:233–241.
- [23]. Da Silva G, Bozzelli JW. J. Phys. Chem. A. 2008; 112:3566–3575. [PubMed: 18348555]
- [24]. Baulch L, Cobos CJ, Cox RA, et al. J. Phys. Chem. Ref. Data. 1994; 23:847–1033.
- [25]. Pitz, WJ.; Seiser, R.; Bozzelli, JW., et al. 2nd Joint Meeting; US Sections of the Combust. Inst. 2001; Paper 253
- [26]. Da Silva G, Bozzelli JW. Proc. Combust. Inst. 2009; 32:287–294.
- [27]. da Silva G, Bozzelli JW. J. Phys. Chem. A. 2009; 113:6979–6986. [PubMed: 19496593]
- [28]. Da Silva G, Hamdan MR, Bozzelli JW. J. Chem. Theory Comput. 2009; 5:3185–3194.
- [29]. Buda F, Bounaceur R, Warth V, Glaude PA, Fournet R, Battin-Leclerc F. Combust. Flame. 2005; 142:170–186.
- [30]. Warth V, Stef N, Glaude PA, Battin-Leclerc F, Scacchi G, Côme GM. Combust. Flame. 1998; 114:81–102.
- [31]. Oehlschlaeger MA, Davidson DF, Hanson RK. Combust. Flame. 2006; 147:195–208.
- [32]. Baulch DL, Bowman CT, Cobos CJ, et al. J. Phys. Chem. Ref. Data. 2005; 34:757–1397.

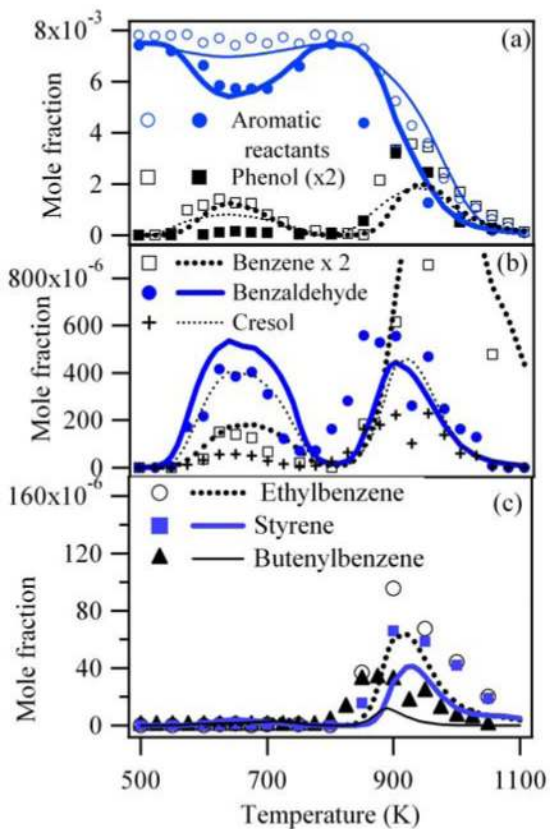


Figure 1.

(a) Mole fractions of the aromatic reactants and phenol vs. temperature for the blends (dark (+toluene) and white (+benzene) points are experiments and thin (+benzene) and thick (+toluene) lines simulations). (b) Mole fractions of the main low-temperature aromatic products vs. temperature for the toluene blend. (c) Mole fractions of the main aromatic products vs. temperature formed only above 800 K for the toluene blend.

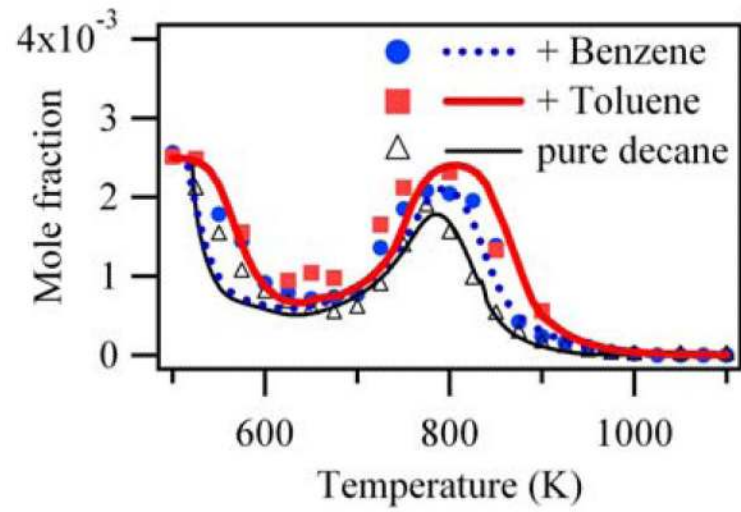


Figure 2.
Mole fractions of *n*-decane vs. temperature.

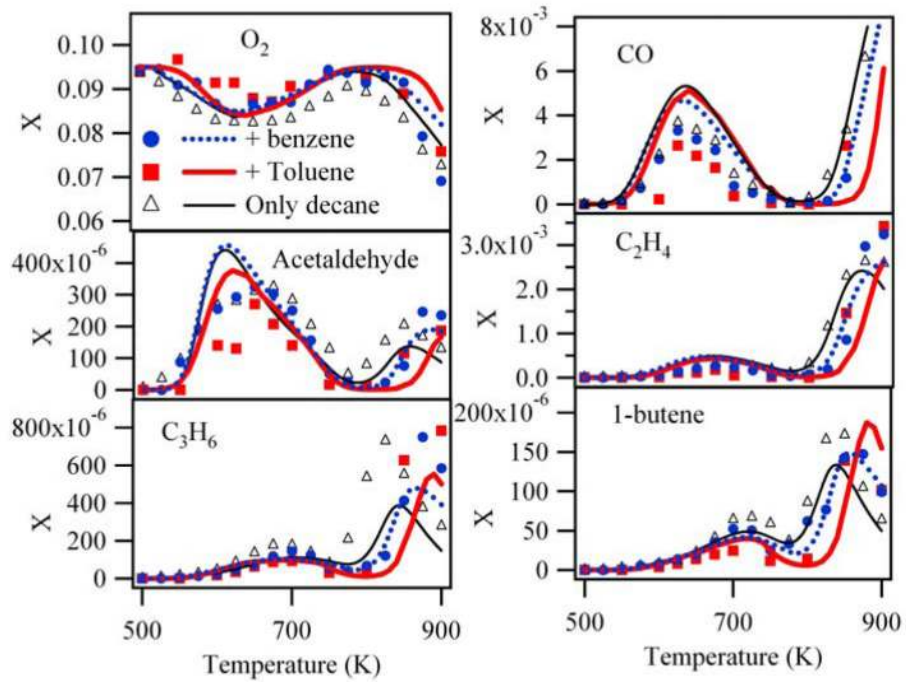


Figure 3. Mole fractions (X) of the major non aromatic species vs. temperature (for a better visualization of the low temperature products, only the 500–900 K range is shown).

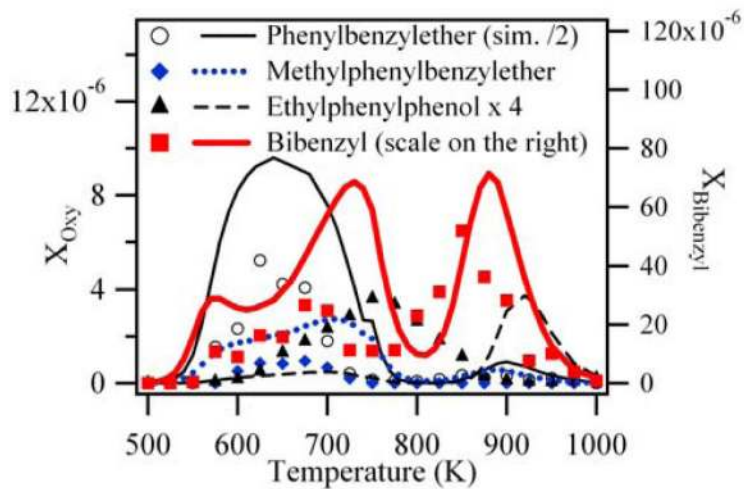


Figure 4. Mole fractions of bibenzyl (X_{Bibenzyl}) and oxygenated diaromatic compounds (X_{Oxy}) vs. temperature for the toluene blend (for a better visualization of the low temperature zone, only the 500-900 K range is shown).

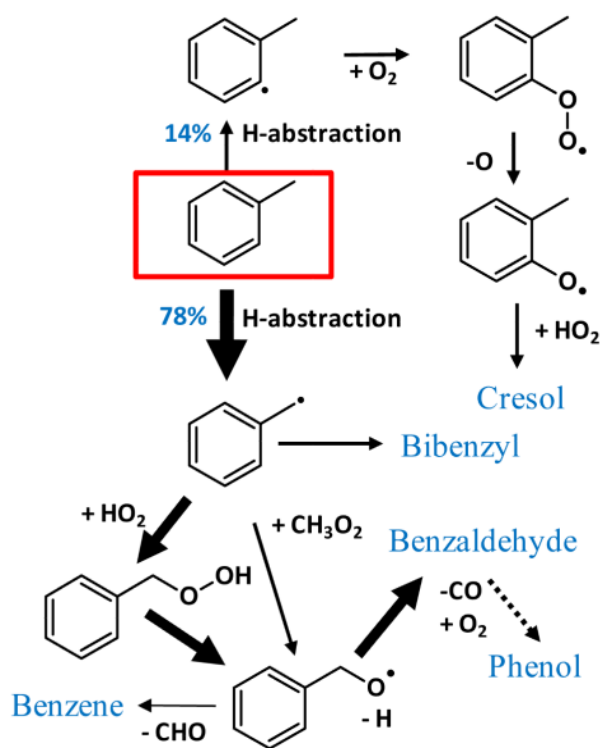
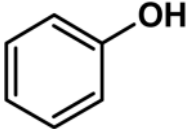
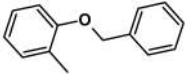
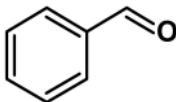
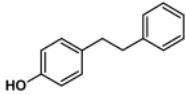
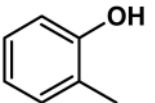
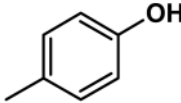
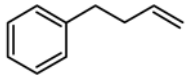
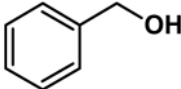
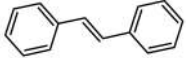
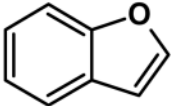
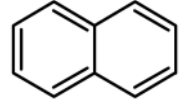
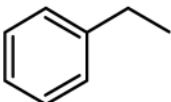
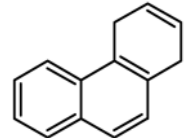
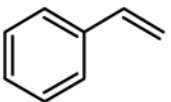
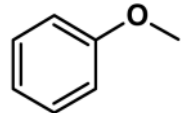
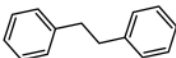
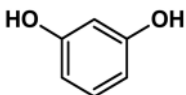


Figure 5. Flow rate analysis for the consumption of toluene (*n*-decane/toluene blend) under the conditions of Fig. 1 at 650 K. The size of the arrows is proportional to that of the flow rates and dotted arrows represent a series of reactions.

Table 1

Names and structures of the aromatic products.

Compound name	Structure	Compound name	Structure
phenol		methyl-phenyl-benzylether	
benzaldehyde		ethyl-phenyl-phenol	
cresols	 	1-butenyl-benzene	
benzylalcohol		stilbene	
benzofuran		naphthalene	
ethyl-benzene		phenanthrene	
styrene		methoxy-benzene	
bibenzyl		hydroxyl-phenol	

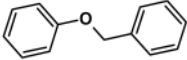
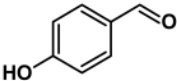
Compound name	Structure	Compound name	Structure
phenyl-benzylether		hydroxyl-benzaldehyde	

Table 2

Changes in the primary mechanisms of the oxidation of benzene and toluene.

Reactions	A	n	E _a	References	n°
C6H5+O2=>C6H5O2 introuvable. (1)	1.86×10 ¹³	-0.22	-0.71	Erreur ! Source du renvoi	
C6H5O2=>C6H5+O2 introuvable. (2)	6.36×10 ¹⁹	-1.37	48.74	Erreur ! Source du renvoi	
C6H5O2=>C6H5O+O introuvable. (3)	1.27×10 ¹⁵	-0.25	38.54	Erreur ! Source du renvoi	
C6H5O2+OOH=C6H5OOH+O2	2.0×10 ¹¹	0.0	-1.3	Estimated ^a (4)	
C6H5OOH=C6H5O+OH	1.5×10 ¹⁶	0.0	43.0	Estimated ^a (5)	
toluene+O2=benzyl+HO2 introuvable. (6)	1.8×10 ¹²	0.0	39.7	Erreur ! Source du renvoi	
toluene+CH3O=benzyl+CH3OH introuvable. (7)	2.12×10 ¹⁰	0.0	3.0	Erreur ! Source du renvoi	
toluene+CH3OO=benzyl+CH3OOH introuvable. (8)	1.02×10 ⁴	2.5	12.3	Erreur ! Source du renvoi	
toluene+C6H5O2=benzyl+C6H5OOH	1.02×10 ⁴	2.5	12.3	Estimated ^b (9)	
benzyl+CH3OO=>C6H5CH2O+CH3O	5.0×10 ¹²	0.0	0.0	Estimated ^c (10)	
benzyl+C2H5OO=>C6H5CH2O+C2H5O	5.0×10 ¹²	0.0	0.0	Estimated ^c (11)	
benzyl+HO2=C6H5CH2OOH introuvable. (12)	8.21×10 ⁴	2.2	-5.13	Erreur ! Source du renvoi	
C6H5CH2OOH=C6H5CH2O+OH introuvable. (13)	3.29×10 ¹³	0.42	39.9	Erreur ! Source du renvoi	
C6H5CH2OOH=C6H5CHO+H2O introuvable. (14)	7.45×10 ⁸	1.19	46.04	Erreur ! Source du renvoi	
C6H5CH2O=RIH+C6H5CHO introuvable. (15)	5.26×10 ²⁸	-5.08	22.2	Erreur ! Source du renvoi	
C6H5CH2O=C6H6#+R5CHO introuvable. (16)	2.37×10 ³²	-6.09	28.8	Erreur ! Source du renvoi	
C6H5CH2O=C6H5#+HCHO introuvable. (17)	7.21×10 ³³	-6.21	36.8	Erreur ! Source du renvoi	
C6H4CH3+O2=>OOC6H4CH3 introuvable. (18)	3.72×10 ¹³	-0.22	-0.71	Erreur ! Source du renvoi	
OOC6H4CH3=>C6H4CH3+O2 introuvable. (19)	6.36×10 ¹⁹	-1.37	48.74	Erreur ! Source du renvoi	
OOC6H4CH3=>OC6H4CH3+O introuvable. (20)	1.27×10 ¹⁵	-0.25	38.5	Erreur ! Source du renvoi	
C6H5CH2OO+H=C6H5CH2O+OH introuvable. (21)	3.8×10 ¹⁴	-0.19	1.89	Erreur ! Source du renvoi	
C6H5CH2OO+H=C6H5CH2OOH introuvable. (22)	4.35×10 ⁶⁰	-15.9	11.4	Erreur ! Source du renvoi	
C6H5CH2OO+H=benzyl+HO2 renvoi introuvable. (23)	1.96×10 ⁴	2.47	1.43	Erreur ! Source du renvoi introuvable. (23)	

Notes: The rate constants are given at 1 atm ($k = A T^n \exp(-E_a/RT)$) in cm^3 , mol, s, kcal units.

^aRate constants taken equal to the values proposed by Buda et al. [29] in the case of equivalent reactions in models of alkanes oxidation.

^bRate constant taken equal to that of reaction (8).

^cRate constants of unimolecular initiations or combinations calculated using software KINGAS [30].